2018 IEEE 15th International Symposium on Biomedical Imaging (ISBI 2018)
April 4-7, 2018, Washington, D.C., USA

Modeling Resting State FMRI Data via Longitudinal Supervised Stochastic Coordinate Coding

Wei Zhang[1], *Jinglei Lv*[1, 2], *Shu Zhang*[1], *Yu Zhao*[1], *Tianming Liu*[1]
[1]Cortical Architecture Imaging and Discovery Laboratory, Department of Computer Science and Bioimaging Research Center, The University of Georgia, Athens, GA, USA; [2]Queensland Institute of Medical Research (QIMR) Berghofer, Herston, OLD, Australia;

ABSTRACT

Resting state fMRI (rsfMRI) has been used widely to explore intrinsic brain activities and networks. Although there are a large number of model-driven and data-driven methods that have been employed to model rsfMRI data, it is challenging to model longitudinal rsfMRI data given the time gaps. Currently, sparse dictionary learning (SDL) method has already shown great promise and attracted increasing attention in the rsfMRI research field. The vital advantage of this SDL methodology is that it can identify concurrent brain networks efficiently and systematically. However, the current SDL is not directly applicable to longitudinal rsfMRI data with multiple time points. In response, we propose a longitudinal supervised stochastic coordinate coding (LSSCC) algorithm for longitudinal rsfMRI data analysis. At the first time point, concurrent brain networks are learned and approximated based on the spatial network templates by SDL with l_2 norm. Then, the learned networks at the first time point are transferred to the following time points and the LSSCC is employed to conduct the approximations of functional networks longitudinally. The application of LSSCC on the ADNI-2 longitudinal rsfMRI datasets has shown the effectiveness of our proposed methods.

Index Terms— resting-state fMRI, stochastic coordinate coding, brain network

1. INTRODUCTION

In the literature, there have been a variety of data-driven methods for modeling resting-state fMRI (rsfMRI) data such as the sparse dictionary learning (SDL) [4], [5]. Despite that multiple novel algorithms for SDL have been developed such as supervised dictionary learning [6], currently, there have been very few SDL methods specifically designed for modeling longitudinal rsfMRI data. Actually, there are many applications that entail novel and effective SDL algorithms to model longitudinal rsfMRI data. For example, Alzheimer's disease (AD) is a typical longitudinal disease and it is urgent to develop effective algorithms that can map the subtle and localized longitudinal changes of brain networks via rsfMRI data [7].

To bridge this technical gap, we propose a longitudinal supervised stochastic coordinate coding (LSSCC) algorithm for longitudinal rsfMRI data modeling. Specifically, at first, we employ the supervised stochastic coordinate coding (SSCC) [8] method to learn the network dictionaries by leveraging the prior knowledge of intrinsic connectivity network (ICN) templates at the first time point. Then, the learned networks at the first time point are transferred to the following time points and then the LSSCC is employed to perform the approximations of longitudinally consistent and smooth ICNs. To evaluate the LSSCC, it is applied on the 30 subjects (30 normal control and 10 AD patients) of ADNI-2 longitudinal rsfMRI datasets and experimental results demonstrated the effectiveness of our proposed methods.

2. METHOD

Our computational framework of LSSCC is summarized in Fig.1. The major novelty and contribution of LSSCC is to enforce the longitudinal consistency and smoothness of network dictionaries in rsfMRI data during the SDL procedure, rather than learning the dictionaries independently in different time points. Detailed steps of our framework are explained in the legend of Fig.1.

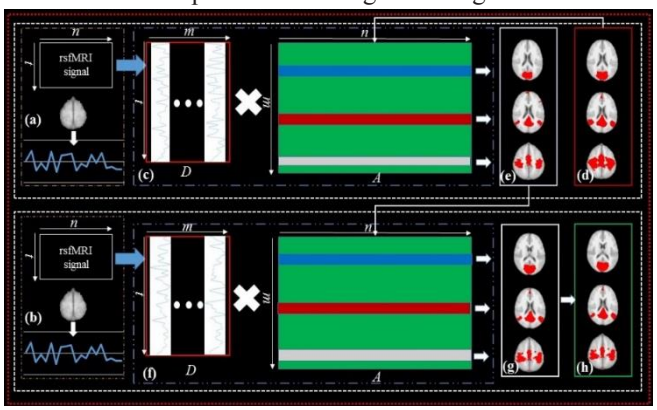

Fig. 1. Illustration of the framework of LSSCC for modeling longitudinal rsfMRI data. (a) rsfMRI signals at the first-time session are extracted and re-organized into 2D signal matrix. (b) rsfMRI signals at the second-time session are similarly extracted and re-organized into 2D signal matrix. (c) the signal matrix at the first-time session is decomposed into a dictionary D and coefficient matrix A; (d) in the first-time scan, the selected ICN templates are employed for smoothing and supervised learning; (e) all identified ICNs from the first-time scan are presented and adopted to perform smoothing and supervised learning in the next time point; (f) the signal matrix at the second-time scan is decomposed into a dictionary D and coefficient matrix A;

(g) LSSCC identifies the longitudinally consistent and smooth ICNs in the current time point; (h) the currently identified ICNs are employed to perform smoothing and supervised learning for the next time point, if available.

2.1. Longitudinal Dictionary Learning Model

If we consider the longitudinal rsfMRI signals from the human brain are represented as $S^T = [s_1^T \ \dots \ \dots \ s_n^T] \in \mathbb{R}^{t \times n}$, $T = 1, 2, \cdots$, where T is the number of total rsfMRI scan sessions for each subject; t is the size of time points in each signal; and n is the voxel number in the brain mask. The objective for LSSCC is to learn a dictionary from the first-time scan session as $D_0 \in \mathbb{R}^{t \times m}$, and a sparse code matrix from the first-time scan session $A_0 \in \mathbb{R}^{m \times n}$, so that each s_i^T is decomposed into a dictionary and a sparse matrix, i.e., $s_i^T = D_T \alpha_i^T$ and the simplified format is $S^T = D^T A^T$ [4], [5]. Given the signal S_i, the traditional dictionary learning problem can be formularized as an optimization problem:

$$minf_i(D, \alpha_i) = \frac{1}{2}\|S_i - D\alpha_i\|_F^2 + \lambda\|\alpha_i\|_1 \qquad (1)$$

where D and a_i are the dictionaries and coefficients, and λ is defined as the regularization parameter to control the sparsity level. The proposed longitudinal dictionary learning model can be designed as two steps. The first step is given the whole-brain rsfMRI data set, the minimization function is formulated as follows:

$$minf_i(D_0, \alpha_i^0) = \frac{1}{2}\left\|S_i^0 - D_0\alpha_i^0\right\|_F^2 + \lambda\left\|\alpha_i^0\right\|_1 + \frac{1}{2}\mu\left\|\alpha_i^0 - TM\right\|_F^2 \qquad (2)$$

where D_0 and α_i^0 are the dictionary and coefficient matrix from the first-time session; TM is the input ICN template used to conduct the smoothing/supervision; μ is considered as the smoothing parameter to control the similarity between the interested coefficient matrix with input templates. Based on our empirical experiments, in this paper, we set λ as 0.1 and μ as 0.6. In the second stage, given the whole brain rsfMRI data, the optimization function is designed as follows:

$$minf_i(D_k, \alpha_i^k) = \frac{1}{2}\left\|S_i^k - D_k\alpha_i^j\right\|_F^2 + \lambda\left\|\alpha_i^k\right\|_1 + \frac{1}{2}\mu\left\|\alpha_i^k - \alpha_i^{k-1}\right\|_F^2, k > 1 \qquad (3)$$

where D_k and α_i^k are the dictionary and coefficient matrix from the k-time point session; μ is considered as the smoothing parameter to control the similarity between the interested coefficient matrix with input templates; α_i^{k-1} is the already learned coefficient matrix from the previous time point session ((k-1)-time session). Based on the optimization models in Eqs. (2) and (3), LSSCC can implement the longitudinal smoothing/supervision to maintain the longitudinal consistency and smoothness for interested ICNs. The implementation details for the LSSCC algorithm are discussed in the next section.

2.2. Longitudinal Supervised Stochastic Coordinate Coding

In this section, we provide the details of the implementation of the proposed LSSCC algorithm. Based on SSCC [8], the dictionaries and coefficient matrices are learned by alternative optimizations. Since the dictionaries' and coefficient matrices' updates are independently, in our proposed LSSCC the process for training dictionaries is the same as SSCC [8]. The major difference here is to update the coefficient matrix based on Eqs. (2) and (3). In the below algorithm 1, we provide the details for updating the coefficient matrix at the first-time scan session; Specifically, Eq (6) uses the gradient descent (GD) to update the element $a_{i,j}^0$ of coefficient matrix; Eq (7) is a shrinkage operation to solve the $l1$ norm problem. Obviously, in this algorithm, at the first-time session, we only concentrate on the identification of interested ICNs, which are similar to the input templates. In both of below algorithms 1 and 2, we employ the conception of *support vector* from SSCC [8].

Algorithm 1 Update $a_{i,j}^0$, the first-time session

1. Perform Coordinate Descent (CD):

$$(a_{i,j}^0)_{it+1} = CD\ (D_i^0,\ (a_{i,j}^0)_{it}, T, s_i^0) \qquad (4)$$

One step of coordinate descent:

for j=1 to m do

$$b_j \leftarrow (a_{i,j}^0)_{it} + \left(d_{i,j}^0\right)^T \times \left(s_i^0 - D_i^0 \times (a_{i,j}^0)_{it}\right) + \mu \times ((a_{i,j}^0)_{it} - TM) \qquad (5)$$

$$a_{i,j}^0 \leftarrow h_\lambda(b_j) \qquad (6)$$

end for

2. Update Support $(a_{i,j}^0)_{it}$
3. Update $(a_{i,j}^0)_{it}$ with certain number of coordinate descent **on the support**:

One step of coordinate descent on the support:

for j=1 to m do

if Support $((a_{i,j}^0)_{it})$=1 do

$$b_j \leftarrow (a_{i,j}^0)_{it} + \left(d_{i,j}^0\right)^T \times \left(s_i - D_i^0 \times (a_{i,j}^0)_{it}\right) + \mu \times ((a_{i,j}^0)_{it} - TM) \qquad (7)$$

$$(a_{i,j}^0)_{it} \leftarrow h_\lambda(b_j) \qquad (8)$$

end if

end for

4. $(a_{i,j}^0)_{it+1} \leftarrow (a_{i,j}^0)_{it}$

In the following stages, we already have the coefficient matrix at the first-time session. Then in Eq.(10), we update the current element $a_{i,j}^k$ from the coefficient matrix by GD. However, the learned element $a_{i,j}^{k-1}$ from the coefficient matrix from the first or last time scan session is used to perform the smoothing/supervision.

Algorithm 2 Update $(a_{i,j}^k)_{it}$ $k \geq 1$, the second/following time sessions

1. Perform Coordinate Descent (CD):

$$(\boldsymbol{a}_{i,j}^{\boldsymbol{k}})_{it} = \boldsymbol{CD}\ (\mathbf{D}_{\mathbf{i}}^{\mathbf{k}},\ (\boldsymbol{a}_{i,j}^{\boldsymbol{k}})_{it}, \mathbf{s}_{i}^{\boldsymbol{k}}) \quad (9)$$

One step of coordinate descent:

for j=1 to m do

$$b_j \leftarrow (a_{i,j}^{k})_{it} + \left(d_{i,j}^{k}\right)^{T} \times \left(s_i^k - D_i^k \times (a_{i,j}^{k})_{it}\right) + \mu \times ((a_{i,j}^{k})_{it} - (a_{i,j}^{k-1})_{it}) \quad (10)$$

$$a_{i,j}^{k} \leftarrow h_{\lambda}(b_j) \quad (11)$$

end for

2. Update Support $(a_{i,j}^{k})_{it}$
3. Update $(a_{i,j}^{k})_{it}$ with certain number of coordinate descent **on the support**:

One step of coordinate descent on the support:

for j=1 to m do

if Support $((a_{i,j}^{k})_{it})$=1 do

$$b_j \leftarrow (a_{i,j}^{k})_{it} + \left(d_{i,j}^{k}\right)^{T} \times \left(s_i^k - D_i^k \times (a_{i,j}^{k})_{it}\right) + \mu \times ((a_{i,j}^{k})_{it} - (a_{i,j}^{k-1})_{it}) \quad (12)$$

$$(\boldsymbol{a}_{i,j}^{\boldsymbol{k}})_{it} \leftarrow \boldsymbol{h}_{\boldsymbol{\lambda}}(\boldsymbol{b}_j) \quad (13)$$

end if

end for

4. $(\boldsymbol{a}_{i,j}^{\boldsymbol{k}})_{it+1} \leftarrow (\boldsymbol{a}_{i,j}^{\boldsymbol{k}})_{it}$

By using the above algorithms 1 and 2, we can update the coefficient matrix from different time points sessions respectively. Then, the dictionary training process from SSCC is employed to update all longitudinal dictionaries independently.

3. RESULTS

The rsfMRI data is obtained from the ADNI-2 data set (http://adni.loni.usc.edu). In this paper, normal control (NC) subjects and AD patients with three different time points of rsfMRI data are employed in our experiments. These rsfMRI datasets were acquired on 3.0 Tesla Philips scanners. A range from 2.29 mm to 3.31 mm of imaging resolution were used in X and Y dimensions. The slice thickness is 3.31 mm. TE (echo time) for all subjects is 30 milliseconds and TR is from 2.2 to 3.1 second. For each subject, there are 140 volumes (time points). The pipeline for ADNI-2 rsfMRI image preprocessing contains skull removal, motion correction, spatial smoothing, temporal pre-whitening, slice timing correction, global drift removal, and band-pass filtering, performed via FSL FEAT. All steps of preprocessing are implemented by FSL FEAT (http://fsl.fmrib.ox.ac.uk). After preprocessing, all images are warped to the MNI template space. In the following sections, we will compare the proposed LSSCC with other two SDL algorithms including the online dictionary learning (ODL) [10] and SSCC [8], using 20 NC subjects and 10 AD patients.

3.1. Comparison of Identified Longitudinal ICNs using ODL, SSCC and LSSCC

In this section, we compare our proposed LSSCC with ODL and SSCC based on the rsfMRI data of NC and AD groups. In Figs.2-3, we provide the identified longitudinal ICN spatial maps by these three methods and the associated qualitative comparisons. By using the widely known visual ICN network and DMN [11] of 20 NC example subjects, in Fig.2, the most three informative slices for NC 1-20 indicate that the identified spatial visual ICN obtained by LSSCC from the first, second and third time points based on NC subjects have stronger longitudinal consistency. However, since ODL decomposes each longitudinal rsfMRI data independently, the identified spatial ICN maps show much less longitudinal consistency. As for SSCC, it shows relatively better longitudinal consistency compared with ODL but less consistency in comparison with LSSCC, based on qualitative analysis.

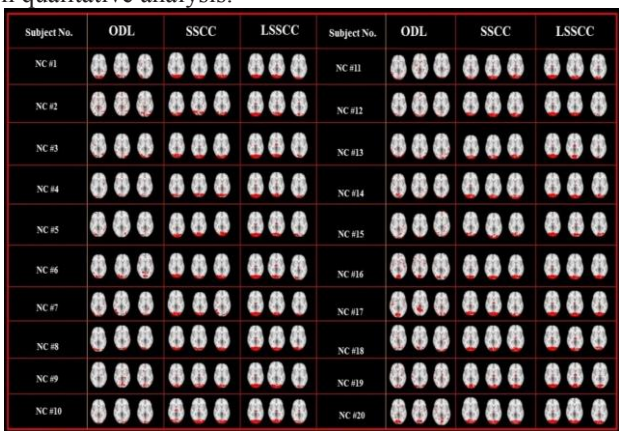

Fig. 2 Qualitative presentation of visual ICN No.2 for 20 NC subjects using ODL, SSCC and LSSCC.

In Fig. 3, we show the results for the identified default mode network (DMN) based on 20 NC subjects.

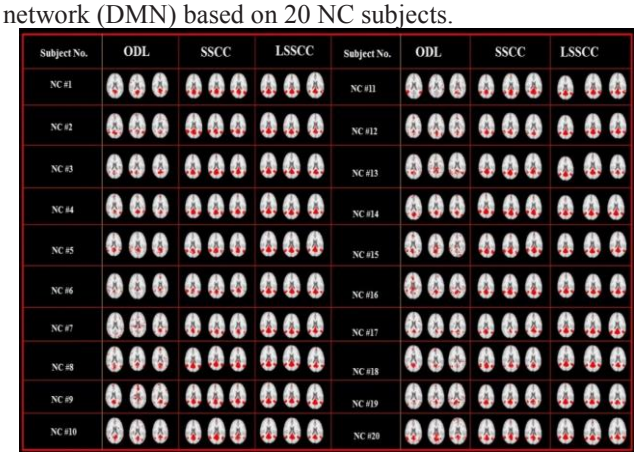

Fig. 3. Identified DMN by ODL, SSCC and LSSCC for 20 NC subjects.

Similarly, in Fig.3, the 3 most informative slices from 3 different time points are presented from the left to the right in each panel, respectively. Based on qualitative analysis of 20 NC subjects, LSSCC and SSCC have better longitudinal

consistency compared with the ODL method. Moreover, LSSCC has a stronger longitudinal consistency than SSCC. For example, in NC #5 and #6, the activated area of DMN identified by SSCC at the first time point (the first slice) is very small, but the activated area from the second time point (the middle slice) become larger; and the activated areas are reduced again in the last slice from the third time point.

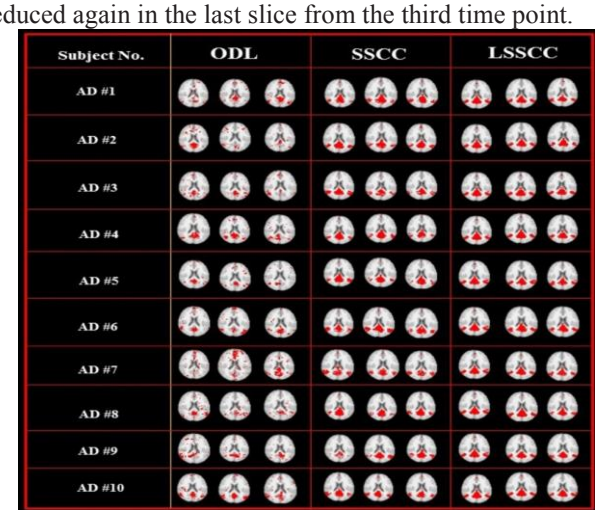

Fig. 4 Qualitative presentation of DMN for 10 AD patients using ODL, SSCC and LSSCC.

In Fig.4, the 3 most informative slices from 3 different time points are presented from the left to the right in each panel, respectively. We provide the identified spatial maps for DMN based on 10 AD patients. The results in the right column indicate that the DMN is consistent through all 3 time points by using LSSCC. Obviously, ODL and SSCC cannot successfully identify the longitudinally robust results, compared with LSSCC, for example, the identified spatial map for AD # 1 by using SSCC. The longitudinal changes for these DMNs are irregular. For instance, the activated areas in DMN at the second-time point are smaller than the activated areas from the first and third-time point.

3.2. Longitudinal Changes of Identified ICNs Mapped by ODL, SSCC and LSSCC

By using a threshold and counting the number of activated voxels in each identified ICN network, we examine the longitudinal changes of ICNs in NC and AD groups, respectively. In Fig. 5, three informative slices of the visual network and DMN from three different time sessions based on NC subject #1, 2 and 3 as the examples are presented and visualized. By qualitative analysis, the longitudinal networks identified by LSSCC for NC group exhibit smoother and more consistent longitudinal changes (the gray curve in Fig.5). In contrast, both ODL and SSCC's results exhibit noisier and non-smooth longitudinal changes (the blue and orange curves in Fig.5). These results suggest the importance of the constraint of temporal smoothness in the dictionary learning in Eq. (3) and demonstrated the advantage of proposed LSSCC method.

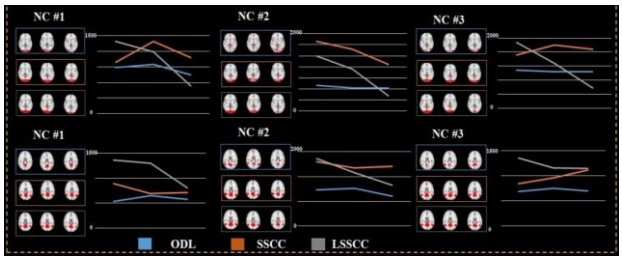

Fig. 5 Longitudinal changes in the visual network and DMN in NC #1, #2 and #3 by ODL, SSCC and LSSCC. Additional visualizations and results of more cases will be provided on our website in the future.

In Fig. 6, we visualized the results for AD patient #1, 2 and 3 as the examples, and compared three methods based on qualitative and quantitatively analysis. Similarly, by using the DMN network as an example, the activated area of DMN identified by LSSCC for AD patient # 1, 2 and 3 exhibit smoother and more consistent longitudinal changes (the gray curve in Fig.6). In contrast, both ODL and SSCC's results exhibit noisier and non-smooth longitudinal changes (the blue and orange curves in Fig.6). These results also suggest the important constraint of temporal smoothness in the dictionary learning in Eq. (3) and demonstrated the advantage of proposed LSSCC method. We believe the results obtained by LSSCC are quite reasonable, since AD is a progressive disease and functional networks are gradually disrupted along the longitudinal time points [7]. This result demonstrated the potential clinical value of our LSSCC method.

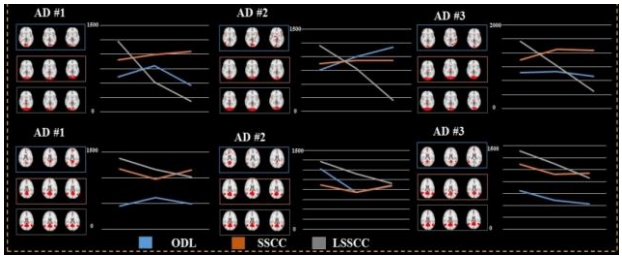

Fig. 6 Longitudinal changes in visual network and DMN for AD subject #1, #2 and #3 mapped by ODL, SSCC and LSSCC. Additional visualizations and results of more cases will be provided on our website in the future.

4. DISCUSSION

In this paper, we proposed a novel longitudinal supervised dictionary learning and sparse representation method named longitudinal supervised stochastic coordinate coding (LSSCC) for modeling longitudinal rsfMRI data. The major novelty and contribution of this work is that we enforce the longitudinal consistency of network dictionaries in rsfMRI data during the SDL procedure, rather than learning the dictionaries independently in different time points. The application of LSSCC on the ADNI-2 longitudinal rsfMRI datasets has shown the effectiveness of our proposed methods. Our work can be

improved in the following directions. First, larger scale AD/NC rsfMRI datasets should be used for evaluation and validation of our methods in the future. Second, the LSSCC can be evaluated and tested in other longitudinal rsfMRI datasets of brain disorders such as Autism. Finally, our LSSCC model should be validated via synthesized rsfMRI datasets with ground truth in the future.

5. REFERENCES

[1] Logothetis, N. K. (2008). What we can do and what we cannot do with fMRI. *Nature*, 453(7197), 869-878.

[2] Thirion, B., & Faugeras, O. (2003). Dynamical components analysis of fMRI data through kernel PCA. NeuroImage, 20(1), 34-49.

[3] Smith, S. M., Miller, K. L., Moeller, S., Xu, J., Auerbach, E. J., Woolrich, M. W., ... & Van Essen, D. C. (2012).

[4] Lv, J., Jiang, X., Li, X., Zhu, D., Zhang, S., Zhao, S., ... & Ye, J. (2015). Holistic atlases of functional networks and interactions reveal reciprocal organizational architecture of cortical function. Biomedical Engineering, IEEE Transactions on, 62(4), 1120-1131.

[5] Lv, J., Jiang, X., Li, X., Zhu, D., Chen, H., Zhang, T., ... & Zhang, J. (2015). Sparse representation of whole-brain fMRI signals for identification of functional networks. Medical image analysis, 20(1), 112-134.

[6] Zhao, S., Han, J., Lv, J., Jiang, X., Hu, X., Zhao, Y., ... & Liu, T. (2015). Supervised dictionary learning for inferring concurrent brain networks. IEEE transactions on medical imaging, 34(10), 2036-2045.

[7] Greicius, M. D., Srivastava, G., Reiss, A. L., & Menon, V. (2004). Default-mode network activity distinguishes Alzheimer's disease from healthy aging: evidence from functional MRI. Proceedings of the National Academy of Sciences of the United States of America, 101(13), 4637-4642.

[8] Lv, J., Lin, B., Li, Q., Zhang, W., Zhao, Y., Jiang, X., ... & Ye, J. (2017). Task fMRI data analysis based on supervised stochastic coordinate coding. *Medical image analysis*, *38*, 1-16.

[9] Liu, J., Yuan, L., & Ye, J. (2010, July). An efficient algorithm for a class of fused lasso problems. In Proceedings of the 16th ACM SIGKDD international conference on Knowledge discovery and data mining (pp. 323-332). ACM.

[10] J. Lv, X. Jiang, X. Li, D. Zhu, H. Chen, T. Zhang, S. Zhang, X. Hu, J. Han, H. Huang, J. Zhang, L. Guo, and T. Liu, "Sparse representation of whole-brain fMRI signals for identification of functional networks.," *Med. Image Anal.*, vol. 20, no. 1, pp. 112–34, Feb. 2015.

[11] Mairal, J., Bach, F., Ponce, J., & Sapiro, G. (2010). Online learning for matrix factorization and sparse coding. Journal of Machine Learning Research, 11(Jan), 19-60.

[12] Smith, S. M., Fox, P. T., Miller, K. L., Glahn, D. C., Fox, P. M., Mackay, C. E., ... & Beckmann, C. F. (2009). Correspondence of the brain's functional architecture during activation and rest. Proceedings of the National Academy of Sciences, 106(31), 13040-13045.